© 2020. Published by The Company of Biologists Ltd | Journal of Cell Science (2020) 133, jcs240705. doi:10.1242/jcs.240705

SHORT REPORT

Efficient genome editing by CRISPR-Mb3Cas12a in mice

Zhuqing Wang[1,*], Yue Wang[1,*], Shawn Wang[1,*], Andrew J. Gorzalski[2], Hayden McSwiggin[1], Tian Yu[1], Kimberly Castaneda-Garcia[1], Brian Prince[1], Hetan Wang[1], Huili Zheng[1] and Wei Yan[1,3,4,‡]

ABSTRACT

As an alternative and complementary approach to Cas9-based genome editing, Cas12a has not been widely used in mammalian cells largely due to its strict requirement for the TTTV protospacer adjacent motif (PAM) sequence. Here, we report that Mb3Cas12a (*Moraxella bovoculi* AAX11_00205) can efficiently edit the mouse genome based on the TTV PAM sequence with minimal numbers of large on-target deletions or insertions. When TTTV PAM sequence-targeting CRISPR (cr)RNAs of 23 nt spacers are used, >70% of the founders obtained are edited. Moreover, the use of Mb3Cas12a tagged to monomeric streptavidin (mSA) in conjunction with biotinylated DNA donor template leads to high knock-in efficiency in two-cell mouse embryos, with 40% of founders obtained containing the desired knock-in sequences.

KEY WORDS: Genome editing, CRISPR, Cas9, Cas12a, Cpf1, PAM

INTRODUCTION

The rapid advancement of CRISPR-Cas-based genome editing technologies has made their clinical applications increasingly promising. However, major obstacles still remain, including safety concerns due to both off-target effects and large on-target deletions or insertions (Adikusuma et al., 2018; Fu et al., 2013; Hsu et al., 2013; Kosicki et al., 2018; Lee and Kim, 2018), and the requirement of proper PAM sequences for efficient and precise cleavage by the commonly used endonucleases, for example, Cas9 and Cas12a/Cpf1 (Komor et al., 2017). The Cas12a endonuclease differs from Cas9 in many aspects and thus, has been considered as an alternative and complementary tool to Cas9. First, the most commonly used *Streptococcus pyogenes* (Sp)Cas9 and Cas12a [*Acidaminococcus* sp. BV3L6 (As)Cas12a and *Lachnospiraceae* bacterium ND2006 (Lb)Cas12a] utilize the NGG and TTTV PAM sequences, respectively, for efficient genome editing (Cong et al., 2013; Jinek et al., 2012; Wang et al., 2013; Zetsche et al., 2015). Second, Cas12a is guided by a single short CRISPR RNA (crRNA), and can efficiently process its own crRNAs, while Cas9 is directed by dual RNAs consisting of a crRNA and a tracrRNA or by a joint large single-guide RNA (sgRNA), and rarely processes its own crRNAs (Cong et al., 2013; Fonfara et al., 2016; Jinek et al., 2012; Zetsche et al., 2017a). Third, Cas12a displays reduced off-target effects compared to SpCas9 due to its irreversible binding to the target region and strong discrimination against off-target sequences (Kim et al., 2017; Kleinstiver et al., 2016; Strohkendl et al., 2018). Finally, Cas9 causes large on-target deletions or insertions (Adikusuma et al., 2018; Kosicki et al., 2018; Lee and Kim, 2018), whereas Cas12a only generates staggered DNA overhangs (Zetsche et al., 2015), which lead to a much lower rate of large on-target deletions or insertions due to the preferred microhomology-mediated end joining (MMEJ) repair mechanism. Despite the advantages, practical applications of Cas12a have been severely hindered due, at least in part, to its strict requirement for the TTTV PAM sequence. Although the PAM sequence for *Francisella novicida* U112 (Fn)Cas12a has been shown to be YTV (Y stands for C/T and V for A/C/G), the actual editing efficiency of the YTV PAM sequences in mammalian cells remains rather low (Tu et al., 2017; Zetsche et al., 2015). Inspired by a recent report suggesting that Mb3Cas12a (*Moraxella bovoculi* AAX11_00205) edits HEK-293 cells at a much higher efficiency through the TTV PAM sequences than does AsCas12a and LbCas12a (Zetsche et al., 2017b preprint), we explored whether Mb3Cas12a could be utilized for efficient genome editing to produce knockout (KO) and knock-in (KI) mouse lines.

RESULTS AND DISCUSSION

To determine whether Mb3Cas12a is active in mouse zygotes, we first tried to use one crRNA harboring a 20 nt direct repeat (DR) sequence with a 20 nt spacer recognizing the TTTV PAM sequence of *Prps1l1* (Table 1; Fig. S1A,D), a testis-specific gene dispensable for spermatogenesis (Wang et al., 2018). One out of six founders obtained had an indel (insertion or deletion) (16.7%) (Table 1; Fig. S1A,D), suggesting that Mb3Cas12a indeed works in mouse zygotes. Previous studies have shown that FnCas12a, AsCas12a and LbCas12a are capable of processing their own crRNAs (Fonfara et al., 2016; Zetsche et al., 2017a), and that residues H843, K852, K869 and F873 in FnCas12a are required for crRNA processing (Fonfara et al., 2016). Given that these four residues are highly conserved among Mb3Cas12a and its three orthologs (FnCas12a, AsCas12a and LbCas12a) (Fig. S1E), we hypothesized that the Mb3Cas12a could also process its own crRNAs. To test this, we designed crRNAs harboring two 20 nt spacers recognizing two TTTV PAM sequences or two TTV PAM sequences at the *Saraf* locus (Table 1; Fig. S1B,F). The 20 nt spacers were separated by two 20 nt DRs. One out of three founders was edited by spacer 1 targeting the TTTV PAM sequence (33.3%) from the first crRNA, and one out of four founders was edited with the spacer 2 (25%) targeting the TTV PAM sequence from the second crRNA (Table 1; Fig. S1B,F). Next, we designed one single crRNA containing two spacers recognizing the TTTV and TTV PAM sequences in the *Mrvi1* locus, respectively (Table 1, Fig. S1C,G). Out of five founders, one was edited with the spacer recognizing the TTTV PAM sequence (20%), but none for the TTV PAM sequence (Table 1; Fig. S1C,G).

[1]Department of Physiology and Cell Biology, University of Nevada, Reno School of Medicine, Reno, NV 89557, USA. [2]Nevada State Public Health Laboratory, University of Nevada, Reno School of Medicine, Reno, NV 89557, USA. [3]Department of Obstetrics and Gynecology, University of Nevada, Reno School of Medicine, Reno, NV 89557, USA. [4]Department of Biology, University of Nevada, Reno, Reno, NV 89557, USA.
*These authors contributed equally to this work

‡Author for correspondence (wyan@med.unr.edu)

Z.W., 0000-0002-3988-0733; W.Y., 0000-0001-9569-9026

Handling Editor: Maria Carmo-Fonseca
Received 15 October 2019; Accepted 18 March 2020

Journal of Cell Science (2020) 133, jcs240705. doi:10.1242/jcs.240705

Table 1. Editing efficiency of Mb3Cpf1 in murine zygotes

Target genes	Length of spacer	No. of spacer in crRNA used	PAM sequence	Site of microinjection	No. of zygotes injected and transferred	No. of newborns (birth rate)[a]	No. of mutants (targeting efficiency)[b]	Indel/ KI	Mono-allelic mutation	Bi-allelic mutation	Multi-allelic mutation
Prps1l1	20 nt	1	TTTV (Spacer 1)	Cytosol (zygote)	22	6 (27.3%)	1 (16.7%)	Indel	Y	N	N
Saraf		2	TTTV (Spacer 1)		22	3 (13.6%)	1 (33.3%)		Y	N	N
			TTTV (Spacer 2)				0 (0%)		N	N	N
		2	TTV (Spacer 1)		21	4 (19%)	0 (0%)		N	N	N
			TTV (Spacer 2)				1 (25%)		Y	N	N
Mrvi1		2	TTTV (Spacer 1)		23	6 (26.1%)	1 (16.7%)		Y	N	N
			TTV (Spacer 2)				0 (0%)		N	N	N
Kcnj10	23 nt	2	TTTV (Spacer 1) and TTV (Spacer 2)	Pronucleus and cytosol (zygote)	39	14 (35.9%)	4 (28.6%)		Y	Y	N
				Cytosol (zygote)	20	13 (65%)	10 (77%)				
miR-10b		3	TTV (Spacer 1)	Cytosol (zygote)	12	5 (41.7%)	1 (20%)		Y	N	N
			TTTV (Spacer 2)				5 (100%)		N	Y	N
			TTTV (Spacer 3)				5 (100%)		N	Y	N
Prps1, *Prps2* and *Prps1l1*		3	TTTV (Spacer 1 targeting *Prps1*)		30	11 (36.7%)	11 (100%)		N	Y	Y
			TTTV (Spacer 2 targeting *Prps2*)				1 (9.1%)		N	Y	Y
			TTTV (Spacer 3 targeting *Prps1l1*)				11 (100%)		Y	N	N
miR-547 and *miR-509*		3	TTTV (Spacer 1 targeting *miR-547*)		38	6 (15.8%)	6 (100%)		N	Y	Y
			TTTV (Spacer 2 targeting *miR-509*)				6 (100%)		N	Y	Y
			TTV (Spacer 3 targeting *miR-509*)				1 (16.7%)		Y	N	N
Slit2		2	TTTV (Spacer 1) TTV (Spacer 2)	Two-cell	23	5 (21.7%)	2 (40%)	KI	N/A		

[a](number of newborns/number of zygotes injected and transferred)×100; [b](number of mutants/number of newborns)×100.

These results suggest that Mb3Cas12a can target genomic DNA with either the TTTV PAM or the TTV PAM sequence.

Although Mb3Cas12a can edit the genome in mouse zygotes, the efficiency appeared to be low. We sought to optimize the editing efficiency by adjusting either the crRNA length or microinjection sites. We first tested the effects of crRNA length on genome editing in the *DNMT1* locus in HEK-293 cells (Fig. 1A,B). No Mb3Cas12a activities were detected when no spacer or a 17 nt spacer was used, whereas the highest Mb3Cas12a activities, comparable to those for AsCas12a and LbCas12a, were observed in the crRNAs with a 23 nt spacer (Fig. 1B). Although FnCas12a uses 21 nt crRNAs more efficiently (Tu et al., 2017), Mb3Cas12a, similar to AsCas12a and LbCas12a, appears to prefer 23 nt crRNAs. We then examined the potential effects of microinjection sites (cytoplasmic versus pronuclear) on targeting efficiency by injecting Mb3Cas12a mRNA and one *Kcnj10*-targeting crRNA harboring two spacers (one recognizing the TTTV PAM sequence, and the other specific for the TTV PAM sequence) into either the cytoplasm or both the pronucleus and cytoplasm of the zygotes. Interestingly, the cytoplasmic-only microinjection yielded more edited mice (77%, n=20) than the combined (pronuclear+cytoplasmic) microinjection (28.6%, n=39) (Table 1, Fig. 1C,D). Taken together, our data suggest that the use of crRNAs with a 23 nt spacer in conjunction with cytoplasmic microinjection represents a highly efficient method to generate indels using Mb3Cas12a in murine zygotes.

To explore whether Mb3Cas12a could target multiple loci simultaneously, we used one crRNA harboring three 23 nt spacers recognizing the TTTV PAM sequences in three *Prps* family genes, including *Prps1*, *Prps2* and *Prps1l1*. Eleven founders obtained were all edited by both the *Prps1* and *Prps1l1* crRNAs (100%), whereas one (9.1%) was edited only by the *Prps2* crRNA (Table 1; Fig. S2A). These results suggest that Mb3Cas12a can indeed process its own crRNAs and edit multiple loci in murine zygotes. Next, we used a crRNA containing three 23 nt spacers separated by three 20 nt DRs to target *miR-10b* (Table 1, Fig. S2B,C). Two of the spacers (spacers 2 and 3) were designed to recognize the TTTV PAM sequence, whereas the other targets the TTV PAM sequence (spacer 1) in the *miR-10b* locus. All five founders were edited by the two spacers targeting the TTTV PAM sequence (100%), and one of them was edited by the one recognizing the TTV PAM sequence (20%) (Table 1; Fig. S2B,C). Moreover, the edited alleles were successfully transmitted to the next generation (Fig. S2D). Similar results were obtained when we used one crRNA containing one 23 nt spacer targeting *miR-547* with the TTTV PAM sequence and two 23 nt spacers targeting *miR-509* with the TTTV PAM and the TTV PAM (Table 1, Fig. 2). All six founders were edited by the two spacers targeting the TTTV PAM sequence (100%), and one of them was edited by the one recognizing the TTV PAM sequence (16.7%) (Table 1, Fig. 2B,C). Although the 23 nt spacers recognizing the TTTV PAM sequence often led to bi- or multi-allelic targeting, and those recognizing the TTV PAM sequence often yielded mono-allelic targeting, the 20 nt spacers appeared to cause mostly mono-allelic mutations (Table 1, Figs 1D, 2C; Figs S1, S2). The mono-allelic targeting may reflect lower Mb3Cas12a editing efficiency when 20 nt spacers or TTV PAM sequences are used. Recent studies have shown that Cas9 with one single gRNA tends to induce large indels in genomic DNA in mouse embryonic stem cells (ESCs), progenitor cells and zygotes (Adikusuma et al., 2018; Kosicki et al., 2018), whereas Cas9 with two gRNAs often causes large deletions within the two flanking gRNA-targeting sites (Wang et al., 2018, 2020).

Journal of Cell Science (2020) 133, jcs240705. doi:10.1242/jcs.240705

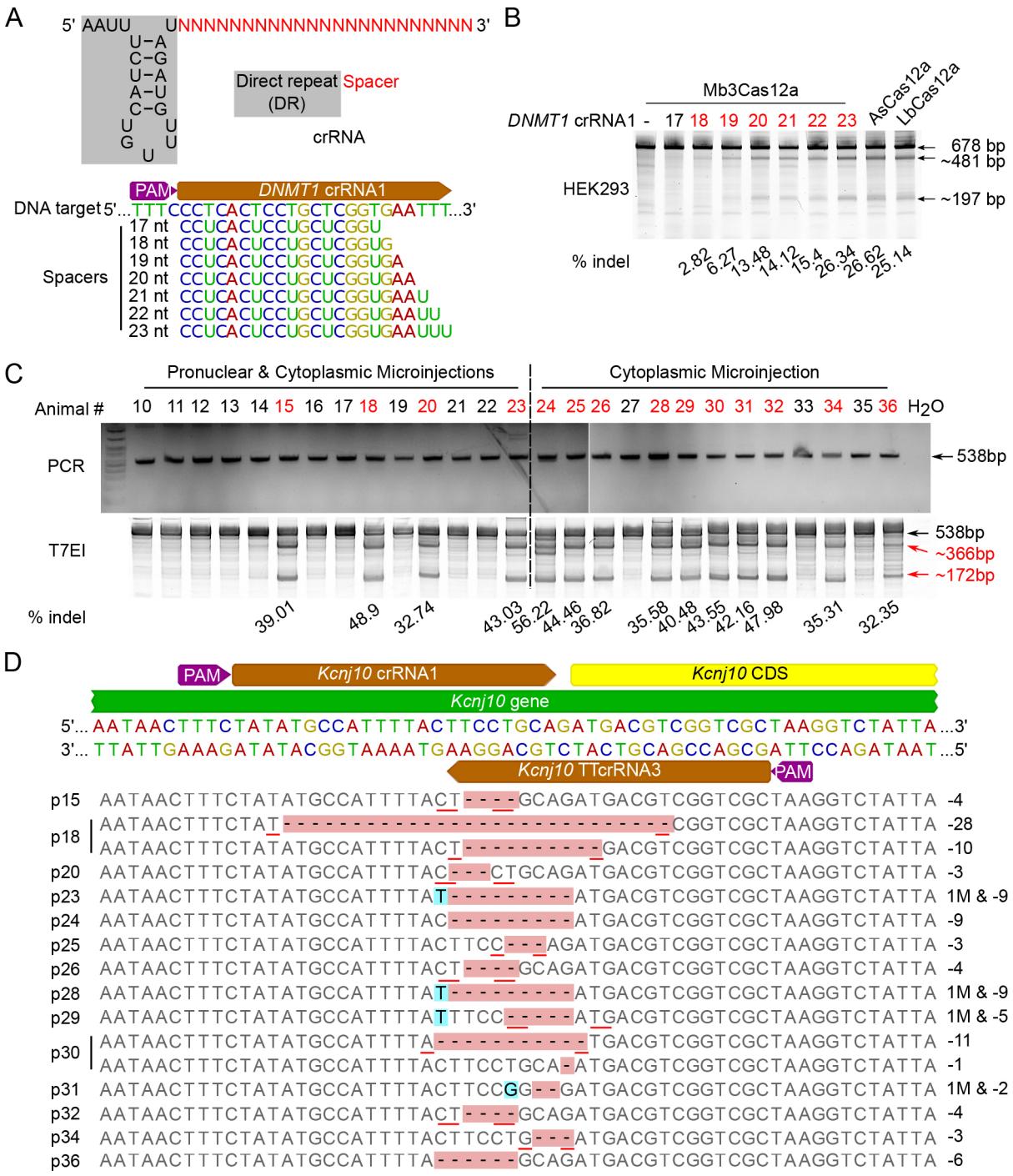

Fig. 1. Optimization of Mb3Cas12a-based genome editing through adjusting crRNA length and microinjection sites. (A) Structure and sequences of the crRNAs used to target the *DNMT1* locus. Upper panel, structure of the crRNAs used, which contain both the 20 nt DR (highlighted in gray) and the 23 nt spacer (red). Lower panel, crRNAs with spacers of variable length, which recognize the TTTC PAM sequences (purple) and were used for targeting *DNMT1* in HEK-293 cells. (B) T7EI assay results of the Mb3Cas12a-edited *DNMT1* locus in HEK-293 cells. The edited samples are shown in red, and AsCas12a and LbCas12a served as positive controls. The sizes of the expected bands after T7EI assays are indicated on the right side of the gel. The percentage of indels are indicated at the bottom of the gel. (C) PCR (upper panel) and PCR-T7EI (lower panel) to identify the efficiency of Mb3Cas12a-based genome editing in the *Kcnj10* locus after either combined pronuclear and cytoplasmic microinjection or cytoplasmic microinjection only in murine zygotes. The edited samples are shown in red. Sizes of the expected bands after T7EI assays are indicated on the right side of the gel. The percentage of indels are indicated at the bottom of the gel. (D) crRNAs used to target *Kcnj10* locus (upper panel) and Sanger sequencing results of Mb3Cas12a-based genome editing in *Kcnj10* locus in murine zygotes (lower panel). Upper panel, PAM sequence is marked in purple, whereas crRNAs are shown in brown. Lower panel, red underlines represent microhomology sequences; the pup number (p) and the total number of edited bases are indicated on the left and the right sides of the Sanger sequencing results, respectively. M, mismatch.

However, Mb3Cas12a-based genome editing appears to generate predominantly indels, because 39 out of the 42 pups derived from Mb3Cas12a-based editing all displayed indels, and only three contained large insertions (7.1%) (Table 1, Figs 1D, 2C; Figs S1, S2). The lack of large on-target insertions or deletions in Mb3Cas12a-based genome editing suggests that the MMEJ mechanism may

Journal of Cell Science (2020) 133, jcs240705. doi:10.1242/jcs.240705

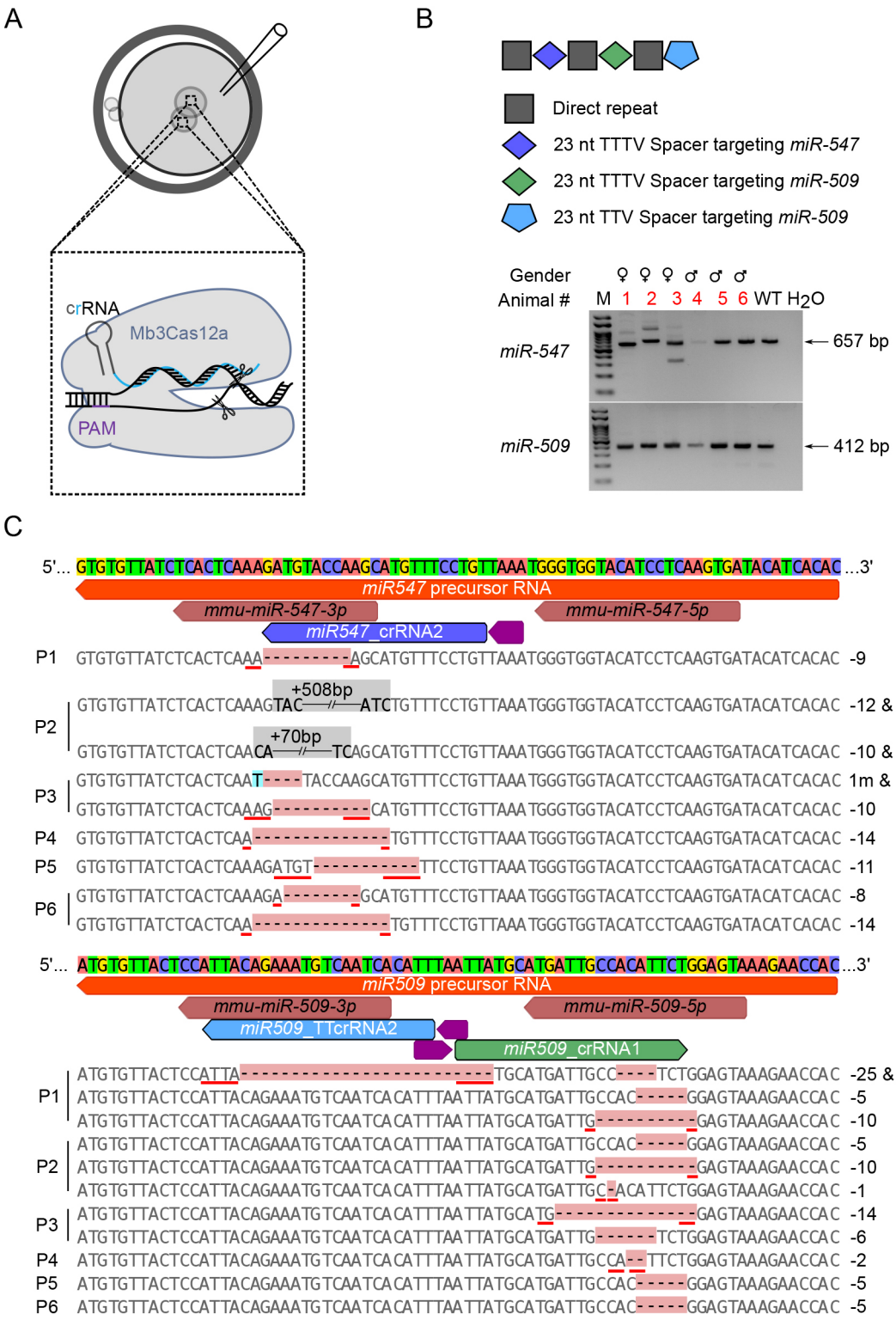

Fig. 2. Multiplex targeting efficiency of Mb3Cas12a-based genome editing in *miR-547* and *miR-509* loci with the TTV PAM sequence in murine zygotes. (A) Schematics showing the strategy used to generate indels in mouse zygotes. Mb3Cas12a mRNA and 23 nt crRNA are microinjected into the cytoplasm of mouse zygotes. The black line represents genomic DNA, purple and cyan lines indicate the PAM sequence and spacer, respectively. (B) PCR genotyping results of Mb3Cas12a-edited *miR-547* and *miR-509* founders. One crRNA with one 23 nt spacer targeting *miR-547* with a TTTV PAM (diamond) sequence and two 23 nt spacers targeting *miR-509* with one TTTV PAM (diamond) and one TTV PAM (pentagon) sequences were used to target the *miR-547* and *miR-509* loci. Squares in gray represent the DR. The edited founders are marked in red, and the corresponding genes and expected band sizes are indicated on the left and right sides of the gels, respectively. (C) Sanger sequencing results of Mb3Cas12a-edited pups 1–6 (P1–P6) at the *miR-547* and *miR-509* loci. Red underlines represent microhomology sequences, whereas the sizes of large insertions are highlighted in gray. Spacers used are marked using the same color as those in B. The PAM sequence is shown in purple. The 508 bp and 70 bp insertions in P2 match a retrotransposon (ERVL-MaLR) and a fragment from the X chromosome (chrX, 67987576–67987641), respectively.

Journal of Cell Science (2020) 133, jcs240705. doi:10.1242/jcs.240705

prefer staggered DNA ends for repair. Interestingly, the large insertions detected in the three founders appeared to be endogenous retroviruses type-L (ERVL) and mammalian apparent LTR retrotransposon (ERVL-MaLR) sequences. A similar phenomenon has been reported in SpCas9-induced double-stranded breaks (DSBs) (Ono et al., 2015), suggesting these retrotransposons may hijack the DSBs induced by either SpCas9 or Mb3Cas12a.

Two-cell homologous recombination (2C-HR)-CRISPR, where Cas9 is tethered with monomeric streptavidin (mSA), which binds to biotinylated DNA donor template, has been shown to have higher KI efficiency (Gu et al., 2018). Given that, we tested whether Mb3Cas12a-mSA could do the same in generating KI mice (Fig. 3A,B). We microinjected two-cell embryos with Mb3Cas12a-mSA mRNA, the *Slit2*-targeting crRNA and the biotinylated DNA donor template (Fig. 3A). Two out of five founders obtained (40%) contained the KI alleles (Fig. 3B,C). In contrast, microinjection of the non-biotinylated donor together with Mb3Cas12a-mSA mRNA and the *Slit2*-targeting crRNA generated no positive founders among 36 pups, although T7EI assays verified that Mb3Ca12a worked (Fig. S3A). These results indicate the Mb3Cas12a-mSA indeed can generate KI mice efficiently.

To test whether Mb3Cas12a could induce off-target effects, we predicted the off-targets using Cas-OFFinder (Bae et al., 2014) and performed T7EI assays on those predicted off-targets. T7EI assays revealed that Mb3Cas12a, just like other Cas12a endonucleases (Kleinstiver et al., 2019; Kocak et al., 2019), also has off-target effects (Fig. S3B–D). Further work is needed to improve its specificity, which may be achieved by either modifying the endonuclease (Kleinstiver et al., 2019) or by using hairpin gRNAs (Kocak et al., 2019). For example, a mutation in enhanced (en)AsCas12a (N282A) can turn it to a high-fidelity endonuclease, whereas a mutation in AsCas12a (R1226A) renders it the nickase that cleaves the non-target DNA

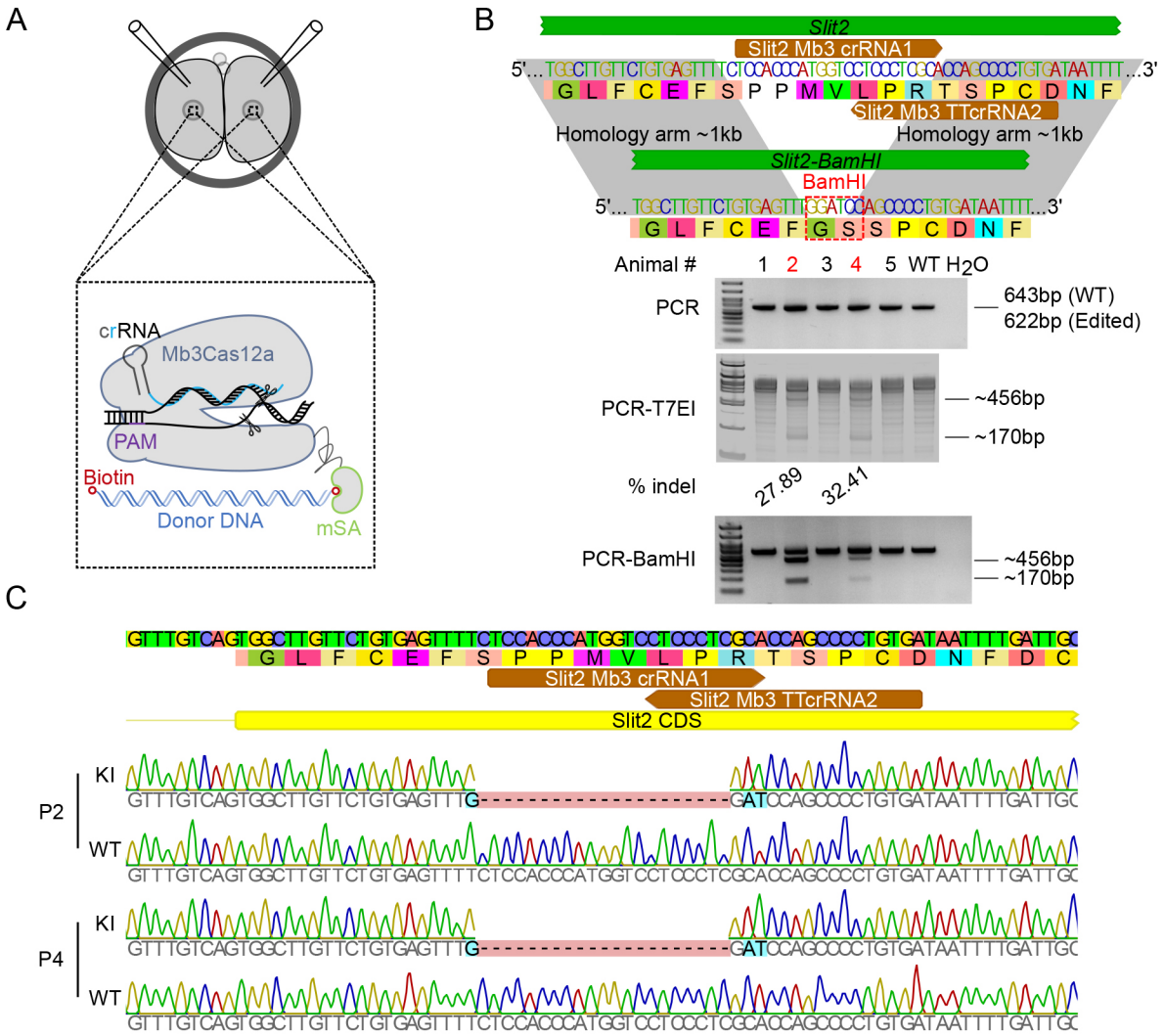

Fig. 3. Generation of a KI in *Slit2* locus using Mb3Cas12a-mSA in mouse two-cell embryos. (A) Schematics showing the strategy used to generate a KI in two-cell mouse embryos. Mb3Cas12a-mSA mRNA, crRNA and biotinylated donor DNA template are microinjected into two-cell mouse embryos. Purple and cyan lines indicate the PAM sequence and spacer, respectively. The blue double-stranded helix indicates the donor DNA with biotin (red open circle). (B) The efficiency of Mb3Cas12a-mSA-mediated KI at the *Slit2* locus in mouse. One crRNA harboring two 23 nt spacers recognizing one TTTV PAM and one TTV PAM sequence was used to target the *Slit2* locus. Upper panel, the strategy used to generate *Slit2-BamHI* KI. The colored characters represent the DNA sequence, and the black characters in colored background indicate corresponding amino acids. Spacers used are shown in brown. The edited BamHI site is shown in red dashed square. Lower panel, PCR, PCR-T7EI (T7 endonuclease I assay) and PCR-BamHI digestion results showing the KI efficiency. The edited founders are indicated in red. The expected band sizes and the percentage of indels are indicated on the right and bottom of the gels, respectively. (C) Sanger sequencing results of Mb3Cas12a-mSA-mediated KI in pups #2 (P2) and #4 (P4) in *Slit2* locus. Spacers used are shown in brown.

strand (Kleinstiver et al., 2019; Yamano et al., 2016). Given that these two residues are conserved between AsCas12a and Mb3Cas12a (Fig. S3E), similar modifications in Mb3Cas12a may also enhance its fidelity, and also lead to the Cas12a version of prime editing, which utilizes the combined Cas9 H840A nickase and MMLV reverse transcriptase activities to minimize off-target effects (Anzalone et al., 2019). In summary, our data demonstrate that Mb3Cas12a can edit the murine genome in a manner that is independent of the TTTV PAM sequence and with minimal on-target mutations and high targeting efficiency. Mb3Cas12a-mediated genome editing expands the toolkit for efficient production of mutant mouse lines.

MATERIALS AND METHODS

Animal use and generation of KO and KI mice

The animal protocol for this study was approved by the Institutional Animal Care and Use Committee (IACUC) of the University of Nevada, Reno (protocol #00494).

All mice were housed and maintained under specific pathogen-free conditions with a temperature- and humidity-controlled animal facility at the University of Nevada, Reno. Generation of KO and KI mice was performed as previously described with modifications (Gu et al., 2018; Wang et al., 2019). Briefly, 4–6-week-old FVB/NJ or C57BL/6J female mice were super-ovulated and mated with C57BL/6J stud males; zygotes and two-cell stage embryos were collected from the oviducts for KO and KI, respectively. For KO, Mb3Cas12a mRNA (200 ng/µl) and crRNA (100 ng/µl) were mixed and injected into the cytoplasm or pronucleus of the zygotes in M2 medium (cat. #MR-051-F, Millipore, Burlington, MA). For KI, Mb3Cas12a-mSA mRNA (75 ng/µl), crRNA (50 ng/µl) and biotinylated donor DNA template (20 ng/µl) were mixed and injected into the cytoplasm or pronucleus of the two-cell stage embryos in M2 medium. After injection, all embryos were cultured for 1 h in KSOM+AA medium (cat. #MR-121-D, Millipore) at 37°C under 5% CO_2 in the air before being transferred into 7–10-week-old female CD1 recipients.

Plasmid construction

To prepare pcDNA3.1-Mb3Cas12a-mSA plasmid, the monomeric streptavidin (mSA) DNA fragment was amplified from PCS2+Cas9-mSA plasmid (Addgene #103882) using Q5® Hot Start High-Fidelity 2X Master Mix (Cat. #M0494S, NEB). The PCR conditions are as follows: initial denaturation at 98°C for 30 s followed by 35 cycles of amplification (denaturation at 98°C for 10 s, annealing at 65°C for 20 s, and elongation at 72°C for 1 min) with the final elongation at 72°C for 2 min. After digestion with BamHI (Cat. #R0136S, NEB, Ipswich, MA) and EcoRI (Cat. #R3101S, NEB) at 37°C for at least 2 h, the digested pY117 plasmid (pcDNA3.1-huMb3Cpf1) (Addgene #92293) and PCR products were purified using Ampure beads and ligated using T4 DNA ligase (Cat. #M0202L, NEB) at 4°C overnight. An aliquot (2 µl) of the ligation products was introduced into 16.7 µl of Mix & Go competent cells (DH5 alpha strain, Cat. #T3007, Zymo Research) for transformation. The transformed cells were spread onto agar plates containing ampicillin (Cat. #BP1760-5, Thermo Fisher Scientific) (100 µg/ml), followed by culture overnight at 37°C. The colonies were picked and genotyped, and the potential positive colonies were cultured overnight in culture medium containing NZCYM broth (Cat. #BP2464-2, Thermo Fisher Scientific) (20 mg/ml) and ampicillin (100 µg/ml). The plasmids were extracted using ZR Plasmid Miniprep (Cat. #D4054, Zymo Research) followed by Sanger sequencing to verify successful cloning. To prepare the pUC-Slit2-BamHI plasmid, two homology arms (~1 kb) flanking the crRNAs cutting sites of *Slit2* locus and pUC empty vector were amplified by Q5® Hot Start High-Fidelity 2X Master Mix (Cat. #M0494S, NEB) from mouse tail genomic DNA and pX330 plasmid (Addgene #42230), respectively. A BamHI restriction site was introduced between the two homology arms through PCR amplification. After purification with Ampure beads, these three DNA fragments were assembled using the NEBuilder® HiFi DNA Assembly Master Mix (Cat. #E2621L, NEB) at 50°C for 1 h. Transformation and verification of ligation were conducted as described above. The primers used for plasmid construction are listed in Table S1.

Generation of Mb3Cas12a and Mb3Cas12a-mSA mRNA, crRNAs and donor DNA template

To synthesize Mb3Cas12a and Mb3Cas12a-mSA mRNAs, the pY117 plasmid (pcDNA3.1-huMb3Cpf1) (Addgene #92293) and pcDNA3.1-Mb3Cas12a-mSA were digested with EcoRI (Cat. #R3101S, NEB) overnight at 37°C, followed by purification with Ampure beads and mRNA synthesis with the HiScribe™ T7 ARCA mRNA kit (Cat. #E2065S, NEB) with addition of a RNase inhibitor (Cat. #M0314L, NEB) at 37°C for at least 2 h. Then the *in vitro* transcribed mRNAs were treated with DNase I (NEB, Cat. #M0303S) to remove the plasmid DNA template, followed by poly(A) tailing using *E. coli* poly(A) polymerase (Cat. #M0276S, NEB) at 37°C for 30 min. The poly(A)-tailed mRNAs were purified using the RNA Clean & Concentrator™-5 (Cat. #R1016, Zymo Research, Irvine, CA) and eluted in a Tris-EDTA solution (Cat.#11-01-02-02, IDT, Coralville, IA).

crRNAs were designed using Benchling (https://benchling.com/). DNA oligonucleotides for making each crRNA were synthesized by the IDT Inc. and are listed in Table S1. To prepare crRNAs for microinjection, the T7 Top strand primer and antisense oligonucleotides specific for each crRNA were mixed in 1× T4 DNA ligase buffer and heated to 95°C for 5 min, and then allowed to cool down to room temperature on the bench. The annealed oligonucleotides were used as the templates for *in vitro* transcription (IVT) using the HiScribe™ T7 High Yield RNA Synthesis Kit (Cat. #E2040S, NEB) at 37°C overnight. After IVT, crRNAs were purified using the RNA Clean & Concentrator™-5 (Cat. #R1016, Zymo Research) and eluted in Tris-EDTA solution (Cat.#11-01-02-02, IDT). To prepare crRNAs for transfection of HEK-293 cells, PCR products corresponding to each crRNA were amplified with U6 forward primer and corresponding antisense oligonucleotides (as listed in Table S1) from the pX330 plasmid (Addgene #42230). After digestion with DpnI (Cat. #R0176S, NEB), the PCR products were purified using Ampure beads. The biotinylated donor DNA template was amplified from the pUC-Slit2-BamHI plasmid with biotinylated primers (as listed in Table S1), followed by DpnI digestion to remove the plasmid and purification with Ampure beads.

HEK-293 cell transfection

HEK-293 cells (Cat. #ATCC® CRL-1573™, ATCC) were maintained in DMEM (Cat. #11995, Thermo Fisher Scientific) containing 10% FBS (Cat. #S12450, R&D Systems) and 1× antibiotic-antimycotic (Cat. #15240062, Thermo Fisher Scientific). At 1 day before transfection, the culture medium was changed to DMEM containing 10% FBS. At ~60% confluence, the HEK-293 cells were co-transfected with 400 ng of pY117 (pcDNA3.1-huMb3Cpf1) (Addgene #92293) and 100 ng of crRNA PCR product using 2.5 µl Lipofectamine 2000 (Cat. #11668, Thermo Fisher Scientific, Waltham, MA) in a 24-well cell culture plate (Cat. #3524, Corning, Corning, NY). The culture medium was changed back to DMEM containing 10% FBS and 1× antibiotic-antimycotic at 12 h after transfection. The cells were collected 48 h after transfection for analyses.

Mouse genotyping and Sanger sequencing

Mouse tail or ear snips were lysed in a lysis buffer (40 mM NaOH, 0.2 mM EDTA, pH 12.0) for 1 h at 95°C, followed by neutralization using the same volume of neutralizing buffer (40 mM Tris-HCl, pH 5.0). PCR was conducted using Platinum™ SuperFi™ Green PCR Master Mix (Cat. #12359010, Thermo Fisher Scientific). The 20 µl PCR mix contained 10 µl of 2× Platinum™ SuperFi™ Green PCR Master Mix, 4 µl of 5× SuperFi™ GC Enhancer, 1 µl of 10 µM forward/reverse primers, 5–50 ng of genomic DNA and nuclease-free water. The PCR conditions were as follows: initial denaturation at 98°C for 30 s, followed by 35 cycles of amplification (denaturation at 98°C for 10 s, annealing at 68°C for 10 s, and elongation 72°C for 1 min) with a final elongation at 72°C for 5 min. Positive samples were subjected to single-A tailing using GoTaq® Green Master Mix (Cat. #M7123, Promega, Madison, WI) for 5 min at 95°C, followed by 15 min at 72°C. The single A-tailed PCR products were then ligated to pGEM®-T Easy Vector using T4 DNA ligase from the pGEM®-T Easy Vector Systems (Cat. #A1360, Promega) at 4°C overnight before transformation. Transformation and verification of ligation were conducted as described in the 'Plasmid construction' section. Data were analyzed using Geneious software (Biomatters, Inc.). The primers used for genotyping are listed in Table S1.

T7EI assay

The T7EI assay (Cat. #M0302L, NEB) was used to detect mutations. PCR products from genotyping were resuspended in 1× buffer 2 and then underwent an initial denaturation at 95°C for 5 min. The denatured PCR products were allowed to anneal by decreasing temperature from 95°C to 85°C with a ramp rate of −2°C/s, followed by a second annealing period from 85–25°C with a ramp rate of −0.1°C/s. The annealed PCR products were then treated with 0.5 µl of T7EI at 37°C for 30 min. The reaction was stopped by adding 0.75 µl of 0.25 M ETDA, as well as 1 µl of Proteinase K (Cat. #P8107S, NEB), followed by incubation at 37°C for 30 min. The T7EI-digested samples (10 µl) were mixed with 2 µl of 6× Purple Gel Loading Dye (Cat. #B7024S, NEB), and loaded into each well of the 10% Novex™ TBE Gels (Cat. #EC62755BOX, Thermo Fisher Scientific) in 1× TBE Buffer (Tris-borate EDTA; Cat. #B52, Thermo Fisher Scientific). The gels were run at 180 V for 30 min, then incubated with 1× TBE buffer containing SYBR Gold (Cat. #S11494, Thermo Fisher Scientific) or ethidium bromide (Cat. #X328, Amresco) for 10 min. The gels were then imaged and analyzed based on the gray density by ImageJ (NIH) and the percentage of indels was quantified as described previously (Cong et al., 2013).

MiSeq library construction and sequencing

Genomic fragments of the *Prps1*, *Prps2* and *Prps1l1* loci were amplified from DNA isolated from mouse tail or ear snips using Platinum™ SuperFi™ Green PCR Master Mix (Cat. #12359010, Thermo Fisher Scientific). The PCR products were then tagged using Nextera XT DNA Library Preparation Kit (Cat. #15032354, Illumina, San Diego, CA) and indexed using Nextera XT Index Kit (Cat. #15055294, Illumina) according to the manufacturer's instructions. Briefly, 5 µl of the PCR product (total 1 ng) were mixed with 10 µl of Tagment DNA (TD) Buffer and 5 µl of Amplicon Tagment Mix (ATM), followed by incubation at 55°C for 5 min. The tagging reaction was then stopped by adding 5 µl of Neutralize Tagment (NT) buffer and incubation at room temperature for 5 min. For indexing, the reaction was mixed with 15 µl of Nextera PCR Master Mix (NPM), 5 µl Index i7 adapters and 5 µl Index i5 adapters, then incubated at 72°C for 3 min. After initial denaturation at 95°C for 30 s, 12 cycles of amplification were performed with the following conditions: denaturation at 95°C for 10 s, annealing at 55°C for 30 s, and elongation at 72°C for 30 s, ending with a final elongation at 72°C for 5 min. After purification with Ampure beads, the DNA library was sequenced using MiSeq Reagent Kit v2 (500-cycles) (Cat. #MS-102-2003, Illumina). Data were analyzed using Geneious software. The primers used for *Prps1*, *Prps2* and *Prps1l1* are listed in Table S1.

Competing interests

The authors declare no competing or financial interests.

Author contributions

Conceptualization: Z.W., W.Y.; Methodology: Z.W., Y.W., S.W., A.J.G., H.M., T.Y., K.C.-G., B.P., H.W., H.Z.; Software: Z.W.; Validation: Z.W., S.W.; Investigation: Z. W., W.Y.; Resources: Y.W., A.J.G., H.Z., W.Y.; Data curation: Z.W., Y.W.; Writing - original draft: Z.W., W.Y.; Writing - review & editing: Z.W., W.Y.; Visualization: Z.W., S.W.; Supervision: W.Y.; Project administration: W.Y.; Funding acquisition: W.Y.

Funding

This work was supported by grants from the National Institutes of Health (HD071736, HD085506 and P30GM110767 to W.Y.) and John Templeton Foundation (PID 61174 to W.Y.). Deposited in PMC for release after 12 months.

Data availability

The datasets generated and/or analyzed during the current study are available in the Sequence Read Archive (SRA) under accession no. PRJNA556550.

Supplementary information

Supplementary information available online at
http://jcs.biologists.org/lookup/doi/10.1242/jcs.240705.supplemental

Peer review history

The peer review history is available online at
https://jcs.biologists.org/lookup/doi/10.1242/jcs.240705.reviewer-comments.pdf

References

Adikusuma, F., Piltz, S., Corbett, M. A., Turvey, M., McColl, S. R., Helbig, K. J., Beard, M. R., Hughes, J., Pomerantz, R. T. and Thomas, P. Q. (2018). Large deletions induced by Cas9 cleavage. *Nature* **560**, E8-E9. doi:10.1038/s41586-018-0380-z

Anzalone, A. V., Randolph, P. B., Davis, J. R., Sousa, A. A., Koblan, L. W., Levy, J. M., Chen, P. J., Wilson, C., Newby, G. A., Raguram, A. et al. (2019). Search-and-replace genome editing without double-strand breaks or donor DNA. *Nature* **576**, 149-157. doi:10.1038/s41586-019-1711-4

Bae, S., Park, J. and Kim, J.-S. (2014). Cas-OFFinder: a fast and versatile algorithm that searches for potential off-target sites of Cas9 RNA-guided endonucleases. *Bioinformatics* **30**, 1473-1475. doi:10.1093/bioinformatics/btu048

Cong, L., Ran, F. A., Cox, D., Lin, S., Barretto, R., Habib, N., Hsu, P. D., Wu, X., Jiang, W., Marraffini, L. A. et al. (2013). Multiplex genome engineering using CRISPR/Cas systems. *Science* **339**, 819-823. doi:10.1126/science.1231143

Fonfara, I., Richter, H., Bratovič, M., Le Rhun, A. and Charpentier, E. (2016). The CRISPR-associated DNA-cleaving enzyme Cpf1 also processes precursor CRISPR RNA. *Nature* **532**, 517-521. doi:10.1038/nature17945

Fu, Y., Foden, J. A., Khayter, C., Maeder, M. L., Reyon, D., Joung, J. K. and Sander, J. D. (2013). High-frequency off-target mutagenesis induced by CRISPR-Cas nucleases in human cells. *Nat. Biotechnol.* **31**, 822-826. doi:10.1038/nbt.2623

Gu, B., Posfai, E. and Rossant, J. (2018). Efficient generation of targeted large insertions by microinjection into two-cell-stage mouse embryos. *Nat. Biotechnol.* **36**, 632-637. doi:10.1038/nbt.4166

Hsu, P. D., Scott, D. A., Weinstein, J. A., Ran, F. A., Konermann, S., Agarwala, V., Li, Y., Fine, E. J., Wu, X., Shalem, O. et al. (2013). DNA targeting specificity of RNA-guided Cas9 nucleases. *Nat. Biotechnol.* **31**, 827-832. doi:10.1038/nbt.2647

Jinek, M., Chylinski, K., Fonfara, I., Hauer, M., Doudna, J. A. and Charpentier, E. (2012). A programmable dual-RNA-guided DNA endonuclease in adaptive bacterial immunity. *Science* **337**, 816-821. doi:10.1126/science.1225829

Kim, H. K., Song, M., Lee, J., Menon, A. V., Jung, S., Kang, Y.-M., Choi, J. W., Woo, E., Koh, H. C., Nam, J.-W. et al. (2017). In vivo high-throughput profiling of CRISPR-Cpf1 activity. *Nat. Methods* **14**, 153-159. doi:10.1038/nmeth.4104

Kleinstiver, B. P., Tsai, S. Q., Prew, M. S., Nguyen, N. T., Welch, M. M., Lopez, J. M., McCaw, Z. R., Aryee, M. J. and Joung, J. K. (2016). Genome-wide specificities of CRISPR-Cas Cpf1 nucleases in human cells. *Nat. Biotechnol.* **34**, 869-874. doi:10.1038/nbt.3620

Kleinstiver, B. P., Sousa, A. A., Walton, R. T., Tak, Y. E., Hsu, J. Y., Clement, K., Welch, M. M., Horng, J. E., Malagon-Lopez, J., Scarfò, I. et al. (2019). Engineered CRISPR-Cas12a variants with increased activities and improved targeting ranges for gene, epigenetic and base editing. *Nat. Biotechnol.* **37**, 276-282. doi:10.1038/s41587-018-0011-0

Kocak, D. D., Josephs, E. A., Bhandarkar, V., Adkar, S. S., Kwon, J. B. and Gersbach, C. A. (2019). Increasing the specificity of CRISPR systems with engineered RNA secondary structures. *Nat. Biotechnol.* **37**, 657-666. doi:10.1038/s41587-019-0095-1

Komor, A. C., Badran, A. H. and Liu, D. R. (2017). CRISPR-based technologies for the manipulation of eukaryotic genomes. *Cell* **169**, 559. doi:10.1016/j.cell.2017.04.005

Kosicki, M., Tomberg, K. and Bradley, A. (2018). Repair of double-strand breaks induced by CRISPR-Cas9 leads to large deletions and complex rearrangements. *Nat. Biotechnol.* **36**, 765-771. doi:10.1038/nbt.4192

Lee, H. and Kim, J.-S. (2018). Unexpected CRISPR on-target effects. *Nat. Biotechnol.* **36**, 703-704. doi:10.1038/nbt.4207

Ono, R., Ishii, M., Fujihara, Y., Kitazawa, M., Usami, T., Kaneko-Ishino, T., Kanno, J., Ikawa, M. and Ishino, F. (2015). Double strand break repair by capture of retrotransposon sequences and reverse-transcribed spliced mRNA sequences in mouse zygotes. *Sci. Rep.* **5**, 12281. doi:10.1038/srep12281

Strohkendl, I., Saifuddin, F. A., Rybarski, J. R., Finkelstein, I. J. and Russell, R. (2018). Kinetic basis for DNA target specificity of CRISPR-Cas12a. *Mol. Cell* **71**, 816-824.e3. doi:10.1016/j.molcel.2018.06.043

Tu, M., Lin, L., Cheng, Y., He, X., Sun, H., Xie, H., Fu, J., Liu, C., Li, J., Chen, D. et al. (2017). A 'new lease of life': FnCpf1 possesses DNA cleavage activity for genome editing in human cells. *Nucleic Acids Res.* **45**, 11295-11304. doi:10.1093/nar/gkx783

Wang, H., Yang, H., Shivalila, C. S., Dawlaty, M. M., Cheng, A. W., Zhang, F. and Jaenisch, R. (2013). One-step generation of mice carrying mutations in multiple genes by CRISPR/Cas-mediated genome engineering. *Cell* **153**, 910-918. doi:10.1016/j.cell.2013.04.025

Wang, Z., Lee, S., Oliver, D., Yuan, S., Tang, C., Wang, Y., Zheng, H. and Yan, W. (2018). Prps1l1, a testis-specific gene, is dispensable for mouse spermatogenesis. *Mol. Reprod. Dev.* **85**, 802-804. doi:10.1002/mrd.23053

Wang, Z., McSwiggin, H., Newkirk, S. J., Wang, Y., Oliver, D., Tang, C., Lee, S., Wang, S., Yuan, S., Zheng, H. et al. (2019). Insertion of a chimeric retrotransposon sequence in mouse Axin1 locus causes metastable kinky tail phenotype. *Mob. DNA* **10**, 17. doi:10.1186/s13100-019-0162-7

Wang, Z., Xie, Y., Wang, Y., Morris, D., Wang, S., Oliver, D., Yuan, S., Zayac, K., Bloomquist, S., Zheng, H. et al. (2020). X-linked miR-506 family miRNAs promote FMRP expression in mouse spermatogonia. *EMBO Rep.* **21**, e49024. doi:10.15252/embr.201949024

Yamano, T., Nishimasu, H., Zetsche, B., Hirano, H., Slaymaker, I. M., Li, Y., Fedorova, I., Nakane, T., Makarova, K. S., Koonin, E. V. et al. (2016). Crystal structure of Cpf1 in complex with guide RNA and target DNA. *Cell* **165**, 949-962. doi:10.1016/j.cell.2016.04.003

Zetsche, B., Gootenberg, J. S., Abudayyeh, O. O., Slaymaker, I. M., Makarova, K. S., Essletzbichler, P., Volz, S. E., Joung, J., van der Oost, J., Regev, A. et al. (2015). Cpf1 is a single RNA-guided endonuclease of a class 2 CRISPR-Cas system. *Cell* **163**, 759-771. doi:10.1016/j.cell.2015.09.038

Zetsche, B., Heidenreich, M., Mohanraju, P., Fedorova, I., Kneppers, J., DeGennaro, E. M., Winblad, N., Choudhury, S. R., Abudayyeh, O. O., Gootenberg, J. S. et al. (2017a). Multiplex gene editing by CRISPR-Cpf1 using a single crRNA array. *Nat. Biotechnol.* **35**, 31-34. doi:10.1038/nbt.3737

Zetsche, B., Strecker, J., Abudayyeh, O. O., Gootenberg, J. S., Scott, D. A. and Zhang, F. (2017b). A survey of genome editing activity for 16 Cpf1 orthologs. *bioRxiv*. doi:10.1101/134015